

Measurement of Fatigue Accumulation in High Strength Steels by Microstructural Examination

Y. G. NAKAGAWA, H. YOSHIZAWA, T. UMEMOTO, C. FUKUOKA
Ishikawajima-Hirata Heavy Industries Co., Ltd., Tokyo, Japan

M. E. LAPIDES
Electric Power Research Institute, Palo Alto, CA USA

ABSTRACT

Fatigue test bars fabricated from a SA508 class 3 low carbon steel plate were cyclicly deformed at 300°C (constant low cycle fatigue, total strain range $\Delta\epsilon=0.78\%$, 0.48%) to crack initiation (100% cumulative damage, CD) and to the factors, 75, 50, and 25% CD. The test bars were, cut perpendicular to the stress axis at the center of the gauge length. The XRD (X-Ray Diffraction line-broadening) was performed on the cross sections created by the cuts. Thin foils ($\sim 0.1\mu\text{m}$ thick) were prepared from each cross section, and used for the TEM and SAD (Selected Area Diffraction) study. The half-value line breadth change measured by the XRD increased with the CD increase up to 50%, beyond which a significant reduction was observed for the 75, and 100% CD sample regardless the incident X-ray beam angle. By the TEM, the undamaged material (0% CD) was characterized by high angle boundaries, small carbide precipitates, and dislocation cell was net works in grains. These characteristics did not show any appreciable changes in all samples with fatigue damage of the respective levels. Micro-orientation changes of the dislocation cells studied by the SAD of the foils and a statistical data analysis clearly demonstrated that the mean orientation difference in the cells, and its standard deviation increased gradually as the CD increased.

1. INTRODUCTION

The objective of the present study is to identify effective methods of measuring the fatigue damage accumulation state in a typical pressure vessel material by microstructural examination. The ASME Boiler and Pressure Vessel Code section III for the design and use of components subject to fatigue in service relies on the standard fatigue test data, namely cyclic strain, S , versus number N cycles, N . The microstructure change in the fatigue process created by induced defects and their distribution in the material would represent a realistic picture of the damage accumulation state, but has not been well investigated for engineering materials¹⁻³. Several techniques for the damage assessment have been found effective to detect cracks and voids, but in general ineffective for detection of microstructural changes due to relatively small

signal/noise ratio. The observations and analyses, tend to be often conflicting in literatures and to date have difficulty in quantifying mechanisms with respect to the fatigue damage accumulation.

It is intended in this paper to demonstrate the capability of the SAD method in quantitative detection of damage.

2. EXPERIMENTAL

Fatigue test bars were machined from a SA508 class 3 low alloy steel plate used for reactor pressure vessels. Fatigue damages were induced in the test bars by constant strain low cycle fatigue with two total strain ranges, $\Delta\epsilon=0.78\%$, 0.48% to crack initiation (100% cumulative damage, CD), and to the factors, 75, 50, and 25% CD. The CD level was determined by the number of cycles relative to that of the crack initiation. The tests were performed in a closed-loop electrohydraulic machine under triangle push-pull strain controlled condition at 300°C . The frequency of cycling was 0.1% strain/sec. The test results are summarized in Table 1.

All the test bars were cut at the center perpendicular to the stress axis. An additional cut was made for the 100% CD bar at the location where the cracking took place. The XRD was conducted on the cross-section planes made by cutting and electro-polishing, measuring line broadening of the diffraction peaks from (211) planes. The equipment used for the XRD was Rigaku-PSPC/MSF system operated at 0.3KW with a $\text{Cr-K}\beta$ target. The measurement was done at incident beam angles, 0, 30, and 45 degree relative to the normal of the cut planes.

Small disks ($3\text{mm}\phi\times 0.1\text{mmt}$) were made from 1mm thick plates cut parallel to the cross sections at which the XRD measurements were done. The foil samples of 2~1000Å thick were prepared by electro-polishing the small disks, and supplied for the TEM and SAD using Hitachi 700H operated at 200KV. The procedure of the SAD method used in this study is schematically illustrated in Figure 1. The SAD was performed inside of grains at $\langle 111 \rangle$ diffraction orientation. In each grain a large number of dislocation cell structures were observed by the TEM as shown in Figure 2. Placing a selector aperture which covered few cell structures, small differences of crystallographic orientation among the cells appeared as small displacement of the diffraction spot, and the pattern was recorded on a negative film. The selector aperture, then, was placed in the neighboring area, and the diffraction pattern was recorded on the same negative. This SAD was repeated five times exposing one negative for diffraction spots of five different areas. The maximum angular deviation, θ , on one negative where the five diffraction patterns were superimposed was measured as seen in Figure 3, and regarded as one data. This five-diffraction superimposition procedure was repeated about twenty times for $\langle 111 \rangle$ oriented grains found in a set of foils made from each fatigue bar at respective CD level, and thus twenty data originated from 100 SAD were collected. A statistical analysis for the data was made by the normal distribution plot from which the mean value and the standard deviation of θ was obtained for each CD.

To compare the microstructure of subsurface layers of the fatigued samples with the bulk microstructure for which all the other TEM and SAD were performed, thin foil samples were made from the surface layers of about 1mm deep of the fatigue tested bars with the 50 and 100% CD.

3. RESULT

The result of the XRD measurement with incident beam angle at 30° for the cross-section planes of the samples fatigued at the two strain levels is illustrated in Figure 4. The diffraction lines with other incident beam angles displayed a similar dependence on the life fraction. The half-value line breadth increased with increasing CD up to 50% beyond which a significant reduction was observed (the 75% and 100% CD sample).

TEM microstructures of the undamaged material (0% CD) was characterized by high angle grain (several μm size) boundaries, carbide precipitates ($\sim 0.1 \mu\text{m}$), and dislocation wall cells ($0.5 \mu\text{m}$) which in some diffraction conditions were observed to be forming columnar parallel net works. The structure was considered to be developed during the heat treatments for the thick plate fabrication. The characteristics of the structure did not show any appreciable changes in the TEM photographs taken from the samples fatigued both at $\Delta\epsilon=0.78\%$ and at $\Delta\epsilon=0.48\%$ with the CD. If there was any, the cell to cell contract increased slightly as the CD increased, which could be noticed only to a TEM expert.

The series of diagrams in Figure 5 are the SAD data expressed in the normal distribution plot for the samples fatigued at $\Delta\epsilon=0.78\%$ of 0, 50, and the near crack of the 100% CD, respectively. One data point represents the maximum angle difference, θ , obtained from one 5-SAD superimposition. The mean value of the difference in the crystallographic orientation of each dislocation cell, θ , and their standard deviations, σ , were obtained from the plots, and the correlations with the CD levels were illustrated together with the lower strain range ($\Delta\epsilon=0.48\%$) fatigue results in Figures 6 and 7, respectively. It can be seen that the statistical distribution of the difference in the crystallographic orientation of each cell is initially narrow (0% CD), and as the CD levels increases the mean value of the difference increases as well as the width of the distribution regardless of the used strain range levels.

4. DISCUSSIONS

The XRD measurement results described in Figure 4 was not clearly understood, but confusing for the fatigue life assessment. One of the reasons is considered to be its inability to differentiate the structural changes occurring in between the macroscopic and the microscopic scale. Since the beam size used for the XRD is in the range of 0.1~10mm diameter, the broadening of the diffraction line is related to integrated changes in the macroscopic strain (sample surface to bulk, grain to grain, formation of the persistent slip bands) as well as in the microscopic strain (in grain, precipitation sub-grains, dislocation, transformation and etc.). This would make the results a rather complex if a major change in the structure is not identified simultaneously. Since there was no significant change observed in the present TEM, the reduction of the line width may have been associated with more macroscopic structural changes, but the detail was yet to be known.

In the present study the TEM microstructures of the subsurface layers about 1mm deep from the surfaces of 50 and 100% CD samples fatigued at $\Delta\epsilon=0.47$ were observed to be close to those of the bulk. It can be concluded that the microstructure have no marked local variation in the samples.

In the TEM microstructure, the initial dislocation cell structure was surprisingly stable, and remained even in the 100% CD sample at the near

crack area. The initial structure was probably brought in through the heat treatments for the plate. Martensitic transformation by quenching induced high dislocation density and the characteristic lath-like structure. The successive tempering and the stress relieving rearranged the dislocations into the net works, yet maintaining the lamella directionality in some of the grains. During fatigue, the flow stress of the sample increases with the number of cycles to a saturation, usually completing hardening at 20~50% CD levels. In this hardening stages, the dislocation density should have increased markedly, but this was not observed by the TEM because the starting material already contained a large number of dislocations, and the newly created dislocations were immediately incorporated into the dislocation bundles (cell walls). It was believed, thus, that major changes, rearrangement of the dislocations, took place in the bundles, were the bundles shook down into fragmented dipoles and prismatic loops. Due to the high dislocation density in the bundles, these structural changes would not be observed even by a high resolution TEM, but would result in the crystallographic microorientation change of the cells. In contrast to the XRD, the SAD supplies crystallographic orientation information from typically 1 μ m diameter area, particularly suited for detecting the misorientation existing among few cells. The results of the present SAD shown in Figure 6 and 7 are encouraging in terms of the fatigue damage assessment since the mean value of the degree of the cell misorientation and the associated standard deviation plotted as a function of the cycles lie close to a single line. In a mechanistic point of view, it is interesting to see if the SAD technique can characterize explicitly the state of 100% CD at which initiated cracks can grow in the structure. Crack initiation is thought to be associated with by macroscopic parameters, large inclusions, surface damages or roughness, and may be excluded from the argument of the microstructural damages.

The SAD technique is currently applied to samples with a composite of cyclic strains simulating a LWR plant service strains to validate this method, and the results will be included in the presentation.

5. CONCLUSIONS

Fatigue test bars fabricated from a SA508 steel plate were cyclically deformed at the two strain amplitude levels ($\Delta\epsilon=0.48\%$, 0.78%) to crack initiation (100% CD) and to 75, 50, and 25% CD. The test bars were cut perpendicular to the stress axis at the center of the gauge length. XRD, TEM, and SAD performed on the cross-sections made by the cuts showed, regardless of the strain amplitude levels, that

1. The half-value line breadth change measured by the XRD peaked at 50% CD yielding no simple correlation with the CD increase.
2. By TEM the undamaged (0% CD) material was characterized by high angle boundaries, small carbide precipitates, and dislocation cell networks in grains. These characteristics did not show appreciable changes in the fatigued samples.
3. Micro-orientation changes of the dislocation cells studied by the SAD and a statistical data analysis demonstrated a gradual increase of the mean cell orientation differences with increasing CD.
4. There was no significant change in the microstructures (TEM and SAD) of the subsurface area from those of the bulk of the fatigued samples.

ACKNOWLEDGMENTS

This research work was performed under the management of the Electric Power Research Institute, Contract No. RP2414-10.

REFERENCES

Lynn, K.G. and Byrne, J.G. (1976). Metall. Trans. A. Vol.7A: pp.604-06.
 Pangborn, R.N., Wissmann, S. and Kramer, I.R. (1979). Proc. 5th Int. Conf. on Strength of Metals and Alloys. Vol.2: pp.1279-84.
 Taira, S. (1973). Exp. Mech. Vol.13: pp.449-63.
 Allen, A.J. Buttle, D.J., Coleman, C.F., Smith, F.A. and Smith R.L. (1988). EPRI Report No. NP5590.
 Coffin, L.F. Jr. (1979). Proc. ASTM-NBS-NSF Symp. on Fatigue Mechanisms. ASTM STP 675. Philadelphia PA: ASTM: pp.9-20.
 Mughrabi, H. (1979). Strength of Metals and Alloys. Vol.3: pp.1615-38.
 Field, J.L. Behnaz F. and Pangborn R.N. (1983) Fatigue Mechanisms. Advances in Quantitative Measurement of Physical Damage. ASTM STP811. Philadelphia PA: ASTM: pp.71-94.

Table 1. Test Results for Fabricating the Fatigue Damage Samples

Specimen Number	Test Temperature (°C)	Total Strain Range, Δε (pct)	Ni Number of Cycles	N Number of Cycles to Crack Initiation	Ni/N Damage Factor
10	300	0.78	2100	2100	1.0
07	300	0.78	1575	—	0.75
09	300	0.78	1050	—	0.50
01	300	0.78	525	—	0.25
03	300	0.48	33,389	33,389	1
05	300	0.48	25,041	—	0.75
06	300	0.48	16,694	—	0.50
02	300	0.48	8347	—	0.25

Frequency of cycling: 0.1 pct/s
 Wave: Strain-controlled push-pull triangle wave

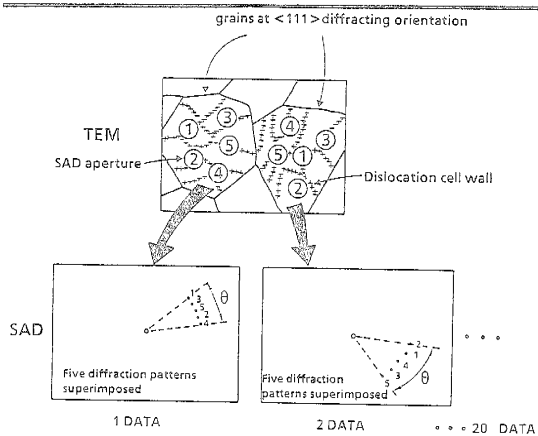


Fig.1 Schematical illustration of the SAD method



Fig.2 Dislocation cell structure observed by TEM

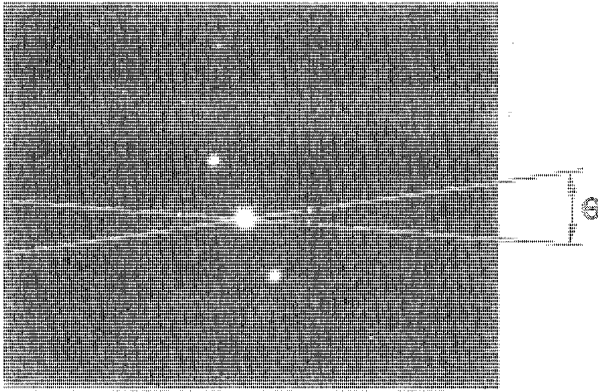


Fig.3 5-diffraction superimposition and measurement of the maximum angular difference

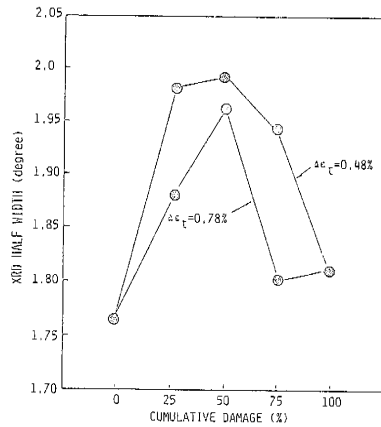


Fig.4 X-ray diffraction half-width as a function of cumulative damage with incident beam angle 30°

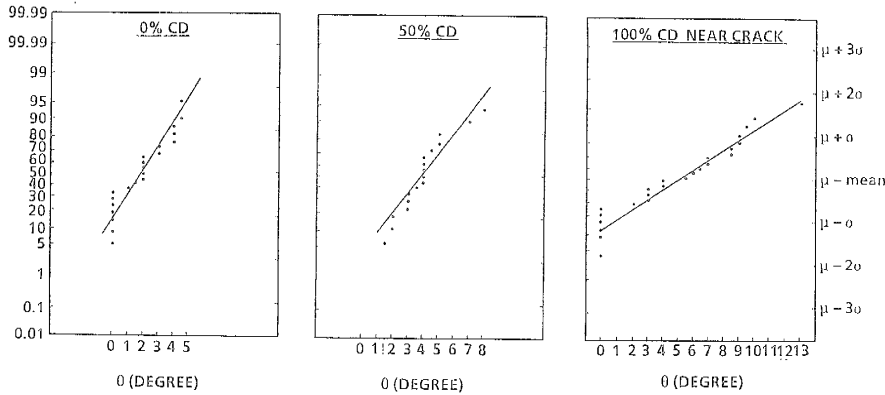


Fig.5 Normal distribution of the difference of the cell orientation, θ , for 0%, 50%, and 100% CD for fatigued

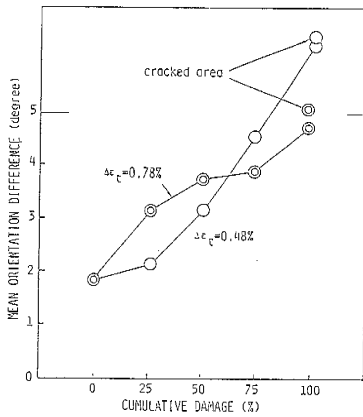


Fig.6 Mean orientation difference of cells measured by SAD as increasing CD

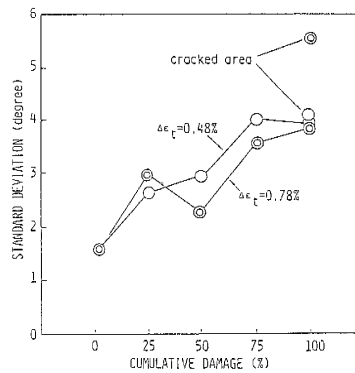


Fig.7 Standard deviation of the cell orientation difference measured by SAD as increasing CD